Mathematical Problems of Computer Science 33, 73–82, 2010.

Automated PAP Algorithm for Interferometric Phase Reconstruction

Yuri A. Barseghyan

Yerevan State University
e-mail: yuri.barseghyan@gmail.com

Abstract

In this work the problem of interferometric phase reconstruction is considered. An automatic windows size selection algorithm is proposed which in combination with earlier developed PAP (pointwise approximation of phase) algorithm provides stable results even for bad quality of interferogramms. Experimental results show that combined algorithm demonstrates better performance in comparison with its original version.

1. Introduction

Many coherent imaging systems utilize the phase coherence between the transmitted and the scattered waves to gather information about the physical and geometrical properties of reflecting objects such as shape, deformation, movement, and structure of the objects surface. Phase estimation plays, therefore, a central role in these coherent imaging systems. For example, in Synthetic Aperture Radar Interferometry (InSAR) the interferometric phase can be used to make extremely fine measurements of surface topography, deformation, or velocity [1, 2, 3]. In adaptive optics the phase measurements provide estimates of atmospheric turbulence effects on an optical imaging system [4, 5, 6]. These atmospheric distortions are then removed through the use of a deformable focusing mirror. In magnetic resonance imaging (MRI) phase measurements from 2-D or 3-D MR images can be used for such purposes as estimating blood flow rates [7] or separating water and fat signals [8, 9].

In all these applications, the *absolute* phase extracted from an actual signal is wrapped into the interval $(-\pi, \pi]$ and called *principal* or *wrapped* phase. If absolute phase value is outside the interval $(-\pi, \pi]$, the observed value of absolute phase is wrapped into this interval by addition or subtraction of some multiples of 2π. The relationship between the wrapped phase ψ and the unwrapped (absolute) phase ϕ is stated as

$$\psi = \phi + 2\pi k, \qquad \psi \in (-\pi, \pi]. \tag{1}$$

In the applications mentioned above the wrapped phase ψ is useless until 2π phase discontinuities are removed, which is realized by using *phase unwrapping* algorithms. Simply stated, the phase unwrapping problem is to obtain an estimate φ for the absolute phase ϕ from the wrapped values ψ.

Measured values of the wrapped phase are usually corrupted by noise which makes phase unwrapping problem more difficult. The phase unwrapping from noisy data starts from the following observation model:

$$z_{\psi} = W(\phi + \Delta\phi), \tag{2}$$

where $\Delta\phi$ denotes a random error additive to ϕ, and z_{ψ} is the observed noisy wrapped phase. W is a wrapping operator transforming the noisy absolute phase $\phi + \Delta\phi$ to the basic interval $(-\pi, \pi]$. The phase unwrapping problem for noisy data is to restore the absolute phase ϕ from the noisy wrapped observations z_{ψ}.

In this paper, we propose new automatic phase reconstruction algorithm based on two independent ideas: ***pointwise approximation*** for design of nonlinear estimators and *adaptation* of these estimators to unknown smoothness of the spatially varying absolute phase. Pointwise polynomial approximation procedure introduced in [10] and called PAP (pointwise approximation of phase) is used for approximation, while the intersection of confidence intervals algorithm (ICI) is used for adaptation.

In the PAP algorithm the pointwise approximation is applied for direct approximation of the absolute phase. For this approximation it uses a polynomial fit in a sliding window. The window size, which was considered in [10] as invariant, and the order of the polynomial define the accuracy of this approximation.

The window size h is a crucial parameter for the accuracy of estimation. When the window size is small, the approximation gives a good smooth fit of signals, but then fewer number of observations are used and the estimates are more variable and sensitive with respect to the noise. Theoretical analysis and experiments show that the efficiency of the local approximation estimates can essentially be improved provided a correct selection of the window size h. Therefore, in this paper the window size is considered as a *varying adaptation variable.*

ICI adaptation algorithm searches for the largest local window size where the variance and the bias of the phase estimates are balanced. It is shown that the pointwise polynomial approximation combined with ICI is efficient and allows to get a nearly optimal quality of estimation in particular for many image processing problems [11]. ICI algorithm returns adaptive windows sizes for each pixel which is giving possibility to automate the PAP algorithm.

2. PAP Algorithm

Let us recall the basic ideas of PAP algorithm [10]. As a observation model we use the following one. Let

$$\phi = \{\phi(x, y) \in \Re, x = 1, ..., N, y = 1, ..., M\}, \tag{3}$$

be the original absolute phase. The observation model is stated as

$$u_1 = \cos\phi + n_1, \quad u_2 = \sin\phi + n_2, \tag{4}$$

where u_1 and u_2 are the so-called *in-phase* (cosine) and *quadrature* (sine) components of the absolute phase ϕ, and n_1 and n_2 are independent white Gaussian noises. Then the wrapped phase g_{ψ} is calculated as follows:

$$g_\psi = \arctan\frac{u_2}{u_1}. \tag{5}$$

We mention that, particularly in optical interferometry and InSAR, the presence of additive white Gaussian noise in the in-phase and quadrature components is in fact the commonly adopted model [12, 13, 14, 15].

If we consider *cos* and *sin* of Equation 1, the difference between wrapped and unwrapped phases disappears ($\cos\psi = \cos\phi$ and $\sin\psi = \sin\phi$) and we can use a fit of these transformed observations for the absolute phase reconstruction. We consider observation in transformed domain (using $cos\psi$ and $sin\psi$) because in phase domain wrapped phase is discontinuous even for a continuous absolute phase because of non-linear characteristics of wrapping operator W. We also assume that the absolute phase $\phi(x, y)$ is a continuous function of the arguments x and y and allows a good polynomial approximation in a neighborhood of the estimation point (x, y).

We assume that observed data is given in phase form (5). Then we calculate

$$g_1 = \cos(g_\psi), \quad g_2 = \sin(g_\psi), \tag{6}$$

which are correspond to transformed noisy observations. According to Equation 2 we can rewrite them in the following form:

$$g_1 = \cos(\phi + \Delta\phi), \quad g_2 = \sin(\phi + \Delta\phi), \tag{7}$$

where $\Delta\phi$ is an error additive to ϕ caused by observation errors in g_ψ.

The local polynomial approximation is applied in order to approximate absolute phase ϕ as an argument of harmonic functions in Equation 7

Let us now introduce estimates of the absolute phase. Assume that in some neighborhood of the point (x, y) the phase $\phi(x, y)$ can be represented in the following form (vector representation of the truncated Taylor series) [11]:

$$\tilde{\phi}(x_s, y_s, P) = Q^T(x_s, y_s)P, \tag{8}$$

where $Q = (q_1, q_2, q_3)^T$ is a vector of first order polynomials $q_1 = 1, q_2 = x, q_3 = y$, and $P = (p_1, p_2, p_3)^T$ is a vector of unknown parameters. The local fit loss function is defined as follows:

$$\begin{aligned} J_h(x, y, P) &= \frac{1}{2}\sum_s \omega_{h,s}\left[g_1(x + x_s, y + y_s) - \cos\tilde{\phi}(x_s, y_s, P)\right]^2 \\ &\quad + \omega_{h,s}\left[g_2(x + x_s, y + y_s) - \sin\tilde{\phi}(x_s, y_s, P)\right]^2 \\ &= \sum_s \omega_{h,s}\left[1 - \cos\left(g_\psi(x + x_s, y + y_s) - \tilde{\phi}(x_s, y_s, P)\right)\right], \\ &\quad \omega_{h,s} = \omega_h(x_s, y_s) \geq 0. \end{aligned} \tag{9}$$

The vector of unknown parameters P is defined as a solution of the following optimization problem:

$$\hat{P} = \arg\min_P J_h(x, y, P). \tag{10}$$

The estimates of the phase ϕ and the first derivatives $\phi_x^{(1)}, \phi_y^{(1)}$ are as follows [11]:

$$\hat{\phi}(x,y) = \hat{p}_1(x,y), \quad \hat{\phi}_x(x,y) = \hat{p}_2(x,y), \quad \hat{\phi}_y(x,y) = \hat{p}_3(x,y). \tag{11}$$

The window $\omega_{h,s}$ defines a set of neighborhood observations and their weights in estimation for point (x,y). The scale parameter h in $\omega_{h,s}$ defines the size of the window and is usually used in the following form: $\omega_h(x,y) = \omega\left(\frac{x}{h}, \frac{y}{h}\right), h > 0$. For example, for the square uniform window $\omega_h = 1$ for $|x| \leq h, |y| \leq h$ and $\omega_h = 0$, otherwise.

Equation 10 shows that we obtain simultaneously the estimates of the phase ϕ and its first derivatives ϕ_x, ϕ_y. These estimates depend on the coordinates (x,y) and the window size h.

Minimization of $J_h(x,y,P)$ with respect to vector P can not be expressed in an explicit form and requires numerical recursive calculations using the vector-gradient: $\partial_P L_h(x,y,P) = (\partial_{P_i} J_h(x,y,P))_{M\times 1}$, and the second derivative (*Hessian*) matrix: $\partial_P \partial_{P^T} L_h(x,y,P) = (\partial_{P_i}\partial_{P_j} J_h(x,y,P))_{M\times M}$, where M denotes the dimension of the vector P (in our case $M = 3$). There are different procedures for calculation of the estimates. We consider the *Newton* method, which can be expressed in the following form:

$$P^{(k+1)} = P^{(k)} - \alpha_k \frac{\partial_p J_h(x,y.P^{(k)})}{H}, \quad k = 0,1,\ldots, \tag{12}$$

where $P^{(k)}$ are sequential iterations of P, $0 < \alpha_k \leq 1$ is the step size parameter, and the gradient $\partial_p J_h$ is calculated for $P = P^{(k)}$.

The straightforward manipulations [10] give the Hessian matrix and the vector-gradient in the form:

$$\partial_P J_h = \sum_s \omega_{h,s} \sin\left(g_\varphi(x+x_s, y+y_s) - \tilde{\phi}(x_s, y_s, P)\right) Q(x_s, y_s), \tag{13}$$

$$H = \sum_s \omega_{h,s} Q(x_s, y_s) Q^T(x_s, y_s). \tag{14}$$

The recursive procedure (12) gives the estimate for any (x,y), provided that in the neighborhood of this point there is sufficient number of observations (x_s, y_s). With independent initialization for each point this is only a denoising algorithm which does not assume the phase unwrapping. Because of that this pointwise estimate is used as an element of a more complex procedure with a special sequence of the estimation points (x,y) arranged with underlying intention to reconstruct continuous phase function $\phi(x,y)$. For instance, it can be a line-by-line sequence. Let us introduce a sequence of the neighboring points $\left\{x^{(n)}, y^{(n)}\right\}_{n=1,\ldots,NM}$ of a rectangular phase data, starting from the point $(1,1)$ and going along the first line, further along the points of the second line, and in a similar way up to the last line. In this way we order all points of the phase data as a sequence.

A straightforward idea of the algorithm is to use for initialization of recursive estimator (12) for the given point (x,y) the estimates already obtained for its neighboring points.

Let $P^{(n)}\left(x^{(n)}, y^{(n)}, P^{(1)}\right)$ be the estimate for the point $\left(x^{(n)}, y^{(n)}\right)$, provided that the recursive pointwise algorithm (12) is initiated by the vector $P^{(1)}$. The proposed phase unwrapping algorithm is defined in the following sequential form:

$$P^{(n)} = P^{(n)}\left(x^{(n)}, y^{(n)}, P^{(n-1)}\right), \tag{15}$$

$$\begin{aligned} \hat{\phi}\left(x^{(n)},y^{(n)}\right) &= p_1^{(n)}, \\ \hat{\phi}_x^{(1)}\left(x^{(n)},y^{(n)}\right) &= p_2^{(n)}, \\ \hat{\phi}_y^{(1)}\left(x^{(n)},y^{(n)}\right) &= p_3^{(n)}, \\ n &= 2,\ldots,N\cdot M. \end{aligned} \tag{16}$$

The recursive pointwise estimator (12) is included in this recursive procedure. It is initiated by the vector $P^{(1)}$, which is the estimate for the first point $\left(x^{(1)},y^{(1)}\right)$. This estimate can be defined from the boundary condition or can be taken from the original observations.

Presented algorithm solves two important goals: noise suppression and absolute phase reconstruction. Experiments show that the accuracy of the algorithm is high provided that the absolute phase differences in the neighboring points are not large than $0.5 \div 1$ radians. The accuracy is as high as small this difference, even for a high level of the random noise.

3. Estimate Accuracy

We rewrite model (7) using linearization in the standard additive-error form:

$$\begin{aligned} g_1 \simeq \cos\phi + \epsilon_1, \quad g_2 \simeq \sin\phi + \epsilon_2, \\ \epsilon_1 = -\Delta\phi\cdot\sin\phi, \quad \epsilon_2 = \Delta\phi\cdot\cos\phi. \end{aligned} \tag{17}$$

According to (5) for (7) we have:

$$g_1 = \frac{u_1}{\sqrt{u_1^2+u_2^2}}, \quad g_2 = \frac{u_2}{\sqrt{u_1^2+u_2^2}}, \tag{18}$$

where u_1 and u_2 are defined by Equation 4. Using Taylor series with respect to small n_1 and n_2, we find that

$$\begin{aligned} z_1 \simeq \cos\phi + \frac{1}{A}\sin^2\phi\cdot n_1 - \frac{1}{A}\sin\phi\cos\phi\cdot n_2, \\ z_2 \simeq \sin\phi - \frac{1}{A}\sin\phi\cos\phi\cdot n_1 + \frac{1}{A}\cos^2\phi\cdot n_2. \end{aligned} \tag{19}$$

Comparing these formulas with equations in (17) we conclude that

$$\Delta\phi = -\frac{1}{A}\sin\phi\cdot n_1 + \frac{1}{A}\cos\phi\cdot n_2. \tag{20}$$

With $E\{n_1\} = E\{n_2\} = 0$ and $var\{n_1\} = var\{n_2\} = \sigma^2$ we find for $\Delta\phi$ that

$$E\{\Delta\phi\} = 0, \quad \sigma_\phi^2 = E\{(\Delta\phi)^2\} = \frac{\sigma^2}{A^2}. \tag{21}$$

So for small noise we can assume that the random $\Delta\phi$ in Equations 7 and 17 is zero-mean with signal independent variance σ_ϕ^2 defined by Equation 21.

The estimation accuracy is calculated as difference between the absolute phase ϕ and the corresponding estimate $\hat{\phi}$: $e_\phi(x,y) = \phi(x,y) - \hat{\phi}(x,y)$. This error consists of two components: the systematic (bias) error corresponding to the deterministic ϕ, and random error corresponding to the random noise ϵ.

We restrict our analysis to the class of smooth differentiable functions with bounded second derivatives

$$\max_{x_s,y_s\in U_h} \left(|\phi_{xx}(x+x_s,y+y_s)|, |\phi_{yy}(x+x_s,y+y_s)|, |\phi_{xy}(x+x_s,y+y_s)|\right) \leq L_2(x,y) \tag{22}$$

where $L_2(x,y)$ is finite and U_h is a support of the window $w_{h,s}$ in (9).

It can be shown that the accuracy of the estimates (11) can be defined for the bias and the variance as follows:

$$|E\left\{e_\phi(x,y)\right\}| \leq \frac{L_2(x,y)\sum_s \omega_{h,s}(|x_s|+|y_s|)^2}{2\sum_s \omega_{h,s}}, \tag{23}$$

$$var\left\{e_\phi(x,y)\right\} \simeq \frac{\sigma^2}{A^2}\frac{\sum_s \omega_{h,s}^2}{\left(\sum_s \omega_{h,s}\right)^2}. \tag{24}$$

4. Automatic Window Size Selection

The Intersection of Confidence Intervals (ICI) rule [16, 17] is an algorithm used for the data driven selection of the window size parameter (close to the optimal) for every point x, y.

The estimates $\hat{\phi_h} = \hat{\phi}\left(x^{(n)}, y^{(n)}\right)$ (16) are calculated for a set $H = \{h_j\}_{j=1}^J$ of increasing windows sizes $h_1 < \ldots < h_J$. The goal of the algorithm is to select among these given estimates $\{\hat{\phi}_{h_j}(x)\}_{j=1}^J$ an adaptive estimate $\hat{\phi}_{h^+}(x), h^+ \in H$, such that $\hat{\phi}_{h^+}(x)$ is close to an "ideal estimate $\hat{\phi}_{h^*}(x)$.

Let us consider a sequence of confidence intervals

$$D_i = \left[\hat{\phi}_{h_i}(x) - \Gamma\sigma_h, \hat{\phi}_{h_i}(x) + \Gamma\sigma_h\right], \tag{25}$$

where $\Gamma > 0$ is a threshold parameter, $\hat{\phi}_{h_i}(x)$ is the estimate of ϕ, σ_h is the standard deviation of the estimate calculated according to Equation 24, $\sigma_h^2 \equiv var\left\{e_\phi(x,y)\right\}$, and i is the index of scale h in H.

The ICI rule defines the adaptive scale as the largest h of those scales in H whose estimate does not differ significantly from the estimates corresponding to the smaller window sizes. Let us consider the intersection of confidence intervals $I_j = \bigcap_{i=1}^j D_i$. Let j^+ be the largest of the indexes j for which I_j is non-empty. Then the optimal scale h^+ is defined as $h^+ = h_{j^+}$ and, as result, the optimal scale estimate is $\hat{\phi}_{h^+}(x)$. Figure 1 illustrates the ICI rule.

The pseudo-code of the combined algorithm (PAP with ICI) is following:

1. **Initialization** of the vector P:
   $P = P^{(1)} : p_1^{(1)} = \psi\left(x^{(1)}, y^{(1)}\right), p_2^{(1)} = \Delta_x\psi\left(x^{(1)}, y^{(1)}\right), p_3^{(1)} = \Delta_y\psi\left(x^{(1)}, y^{(1)}\right),$
   where ψ is the observed wrapped phase.
2. **For every point of the sequence** $\left(x^{(n)}, y^{(n)}\right), n = 2, \ldots, N_xN_y$ **:**

(a) calculate the vectors $P^{(n)}$ and the pointwise estimates $\hat{\phi}_h^{(n)}$ according appropriate Equations 12, 14, 15-16;

(b) repeat calculations for all $h = h_1, h_2, \ldots$;

(c) apply the ICI rule for selection of the best window size and the adaptive window size estimate $\hat{\phi}_{h^+}^{(n)}$.

The **Initialization** is used only for the first point $\left(x^{(1)}, y^{(1)}\right)$.

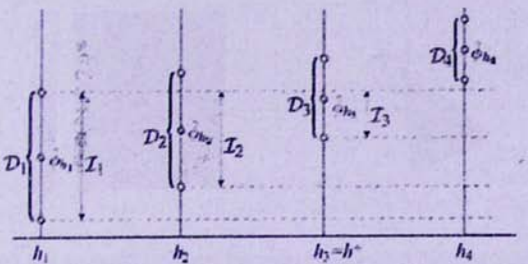

Figure 1. Illustration of ICI rule.

5. Experimental Results

For the accuracy measurements of the developed algorithm we use the root-mean-squared-error: $RMSE = \sqrt{\frac{1}{N_x N_y} \sum \left(\phi(x_s, y_s) - \hat{\phi}(x_s, y_s)\right)^2}$. With the PAP we use the uniform square windows ω_h defined on the integer grid $U_h = \{x, y : x = -h, -h+1, \ldots, 0, \ldots, h-1, h, y = -h, -h+1, \ldots, 0, \ldots, h-1, h\}$. For ICI algorithm we use $\Gamma = 2$.

The Pyramidal absolute phase test function, presented in Figure 2 (a), is defined by the following formulas:

$$\begin{aligned} &\phi(x, y) = \frac{1}{2} \cdot \min(\phi_1, \phi_2, \phi_3, \phi_4), \\ &\phi_1 = x, \quad \phi_3 = 255 - x, \\ &\phi_2 = y, \quad \phi_4 = 255 - y, \end{aligned} \tag{26}$$

considered on the integer grid $x = (0 : 255), y = (0 : 255)$, The maximum value of the absolute phase ϕ is equal to 63.5 radians. The maximum difference between pixels is equal to 0.5 radians.

Figure 2 illustrates the original absolute phase ϕ (a) and noisy wrapped phase g_ψ (b) obtained from ϕ according to Equation 5, with the standard deviation of the white Gaussian noise $\sigma = 0.4$. This figure also presents result of the reconstruction using PAP algorithm combined with ICI rule (c) and the absolute errors of the phase reconstruction (d). Comparing the original and reconstracted phases, one may conclude that the noise suppression and phase reconstruction is performed quite accurately.

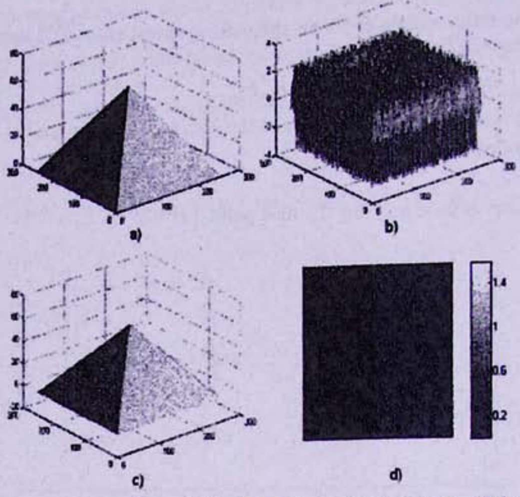

Figure 2. a) Original absolute phase ϕ, b) observed wrapped phase g_{ψ} with additive white Gaussian noise, c) reconstructed phase $\hat{\phi}$, d) absolute errors of reconstruction.

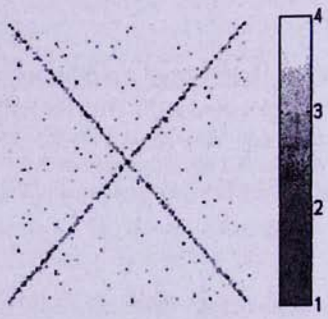

Figure 3. ICI adaptive window sizes for Pyramid phase.

The adaptive window sizes shown in Figure 3 give insight how the adaptation works. Mainly, the largest window size is selected excluding the areas near pyramid edges, where the adaptive window size takes the minimum value. In this way, the algorithm enables the maximum smoothing of the noise for the flat surfaces where the used linear model perfectly fits to the surface and the maximum window size can be used. For the edges, small window size allows to avoid the surface oversmoothing, however, at the price of a higher level of random errors. The effect of the varying window selection is illustrated also by the last image in Figure 2 (d) showing the absolute errors of the phase reconstruction. These errors are minimal on flat surfaces of the pyramid where the window sizes take maximal values and these errors are maximal along the pyramid edges where the adaptive window sizes are minimal.

Table below presents the numerical evaluation of the algorithm performance. For estimation we use different windows sizes $h = \{1, 2, 3, 4\}$ and different values of standard deviation σ of the white Gaussian noise in Equation 4. We can see a difference between the estimates with invariant h and varying adaptive one. In all cases, the combined algorithm enables minimization of RMSE values and even slightly better results that the best one achieved for the invariant window size.

Algorithm/σ	.1	.2	.3	.4	.5
PAP, h=1	.040	.072	.109	.152	.199
PAP, h=2	.048	.060	.077	.099	.124
PAP, h=3	.071	.076	.084	.095	.109
PAP, h=4	.100	.102	.106	.111	.120
PAP, ICI	**.028**	**.052**	**.071**	**.091**	**.111**

In our first paper [10], phase reconstruction is produced with a fixed window size. In combined algorithm, presented in this paper, the phase reconstruction is performed on the estimates with already adaptive windows sizes. Comparison of the algorithms is definitely in favor the combined algorithm (PAP with ICI) which demonstrates much better performance and stable results.

References

[1] Graham L. C. "Synthetic interferometer radar for topographic mapping". *In Proceedings of the IEEE*, 1974, v. 62, p. 763.

[2] Goldstein R. M., Zebker H. A., Werner C. L. "Satellite radar interferometry: Two-dimensional phase unwrapping". *Radio Science*, 1997, v. 23, p. 713.

[3] Ghiglia D. C., Eichel P. H. "High-resolution synthetic aperture radar interferometry: Technology for precise terrain elevation mapping". *DSP and Multimedia Technology*. 1994, v. 3.

[4] D. L. Fried. "Least-squares fitting a wave-front distortion estimate to an array of phase-difference measurements". *Journal of the Optical Society of America*, 67(3):370-375, March 1977.

[5] W. W. Arrasmith, M. C. Roggemann, B. M Welsh. "Optimal Wave-front Reconstruction for a Coherent Diffracted Field". *Applied Optics*, 37(20):4457-4467, 1998.

[6] R. J. Noll. "Phase estimates from slope-type wave-front sensors". *Journal of the Optical Society of America*, 68(1):139-140, January 1978.

[7] A. Herment, E. Mousseaux, O. Jolivet, A. DeCesare, F. Frouin, A. Todd-Pokropek, J. Bittoun. "Improved Estimation of Velocity and Flow Rate Using Regularized Three-Point Phase-Contrast Velocimetry". *Magnetic Resonance in medicine*, 44:122-128, 2000.

[8] M. Hedley, D. Rosenfeld. "A new Two-Dimensional Phase unwrapping Algorithm for MRI Images". *Magnetic Resonance in Medicine*, 24:177-181, 1992.

[9] G. H. Glover, E. Schneider. "Three-Point Dixon Technique for True Water/Fat decomposition with B_0 Inhomogeneity Correction". *Magnetic Resonance in Medicine*, 12:371-383, 1991.
[10] Y.A. Barseghyan "Pointwise Reconstruction of Interferometric Phase". *Mathematical Problems of Computer Science*, vol. 32, pp. 48-55, 2009.
[11] Katkovnik V., Egiazarian K., Astola J. "Local approximation techniques in signal and image processing". *SPIE PRESS*, Bellingham, Washington, 2006.
[12] K. Ho and J. Kahn, "Exact probability density function for phase measurement interferometry". *J. Opt. Soc. Amer. A*, vol. 12, pp. 1984-1989, 1995.
[13] J. Lee, K. Hoppel, S. Mango, and A. Miller. "Intensity and phase statistics of multilook polarimetric and interferometric SAR imagery". *IEEE Trans. Geosci. Remote Sensing*, vol. 32, pp. 1017-1028, 1994.
[14] S. Madsen, "Spectral properties of homogeneous and nonhomogeneous radar images", *IEEE Trans. Aerosp. Electron. Syst.*, vol. AES-23, pp. 583-588, 1987.
[15] C. Rathjen, "Statistical properties of phase-shift algorithms". *J. Opt. Soc. Amer. A*, vol. 12, pp. 1997-2008, 1995.
[16] A. Goldenshluger and A. Nemirovski, "On spatial adaptive estimation of nonparametric regression", *Mathematical Methods of Statistic*, vol. 6, pp. 135-170, 1997.
[17] V. Katkovnik, "A new method for varying adaptive bandwidth selection". *IEEE Transactions on Signal Processing*, vol. 47, no. 9. pp. 2567-2571, 1999.

Ավտոմատացված PAP ալգորիթմ ինտերֆերոմետրիկ փուլի վերականգնման համար

Յ. Բարսեղյան

Ամփոփում

Աշխատանքում քննարկվում է ինտերֆերոմետրիկական փուլի վերականգնման խնդիրը: Առաջարկվում է պատուհանի չափսի ընտրման ավտոմատացված ալգորիթմ, որը միավորված մինչ այդ ստեղծված PAP ալգորիթմի հետ ապահովում է կայուն արդյունքները նույնիսկ ինտերֆերենցիոն պատկերների վատ որակի դեպքում: Փորձերի արդյունքները ցույց են տալիս, որ միավորված ալգորիթմը է համեմատած նախնական ալգորիթմի հետ, տալիս է փուլի վերականգնման ճշտության զգալի լավացումը: